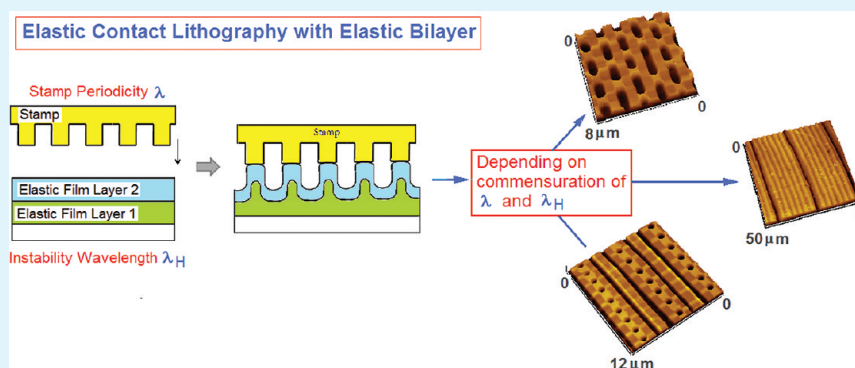


Creating Self-Organized Submicrometer Contact Instability Patterns in Soft Elastic Bilayers with a Topographically Patterned Stamp

Rabibrata Mukherjee*[†] and Ashutosh Sharma*[‡]

[†]Department of Chemical Engineering, Indian Institute of Technology, Kharagpur, 721 302, India, and [‡]Department of Chemical Engineering and DST Unit on Soft Nanosciences, Indian Institute of Technology, Kanpur, 208 016, India

S Supporting Information



ABSTRACT: The surface of a thin elastic bilayer becomes spontaneously unstable when it is brought in proximity to another rigid contactor. The instability patterns, which are random and isotropic, exhibit a dominant lateral length scale of instability λ , which linearly scales with the bilayer thickness (h) as: $\lambda = R_F h$. It is known that for an elastic bilayer, R_F exhibits a nonlinear dependence on the ratios of individual film thicknesses (H) and shear moduli (M) of the two constituent layers, and can have values as low as 0.5 under specific conditions. This is in contrast to a near constant value of $R_F \approx 3$ for a single layer elastic film.¹ These isotropic contact instability patterns in a bilayer can be ordered, aligned and modulated using a topographically patterned stamp. The precise morphology of the aligned structures depends on commensuration between λ and the stamp periodicity (λ_p), and on the intersurface separation distance. A variety of patterns, like an array of circular holes, double periodic channels, etc., in addition to a positive and a negative replica of the stamp pattern, can be engineered with a simple stamp having 1D grating structure. A lower value of R_F in a bilayer allows generating patterns with sub 500 nm lateral resolution, which is impossible to create by elastic contact lithography (ECL) of a single layer film due to strong surface tension effects in ultrathin films. Thus, control of elastic instability in a bilayer with a patterned stamp represents a flexible soft lithography tool allowing modulation of length scales, morphology, and order.

KEYWORDS: self organization, bilayer, patterns, elastic film, soft lithography, thin film instability

INTRODUCTION

The free surface of a thin soft solid film exhibiting room-temperature elasticity becomes unstable and forms isotropic labyrinth like structures when it is brought in contact proximity with another rigid surface, which has been studied both experimentally, and theoretically.^{1–40} Reduction in the total free energy of the elastic bilayer engenders self-organized pattern formation owing to the attractive adhesive interactions with a contact surface or stamp.^{1–34} Experimentally, this system has been studied in several geometries, using either a rigidly bonded convex contactor,^{2,3,8} or flexible contactor peeled from one side,^{3,4,10,11,13,15} or a flat rigid contactor parallel to the film surface.^{1,5,22} The problem has also been investigated theoretically^{6,8,12,14,17,18} based on linear stability analysis (LSA) as well as nonlinear simulations to predict morphologies during bonding and debonding. The length scale of the instability is obtained by the minimization of the stored elastic strain

energy.^{2,9,12} Similar instability is also observed when an external field is applied across a soft elastic film.^{36–40} This particular form of instability involves only elastic deformations and does not involve any flow or transport of material by diffusion or convection. It is thus distinct from the long wave instability in ultrathin viscous liquid films due to van der Waals interaction,^{41–48} electric field,^{49,50} thermal gradient,^{51,52} release of residual stresses,^{53,54} density variation,⁵⁵ etc. It is also different from the classical Saffman–Taylor instability observed in a Hele Shaw cell.⁵⁶ Although some of the patterns are morphologically similar, this form of instability is also distinct from thermo-capillarity-induced pattern formation in a film subject to a large transverse thermal gradient,⁵⁷ or wrinkling of

Received: October 16, 2011

Accepted: December 9, 2011

Published: December 9, 2011

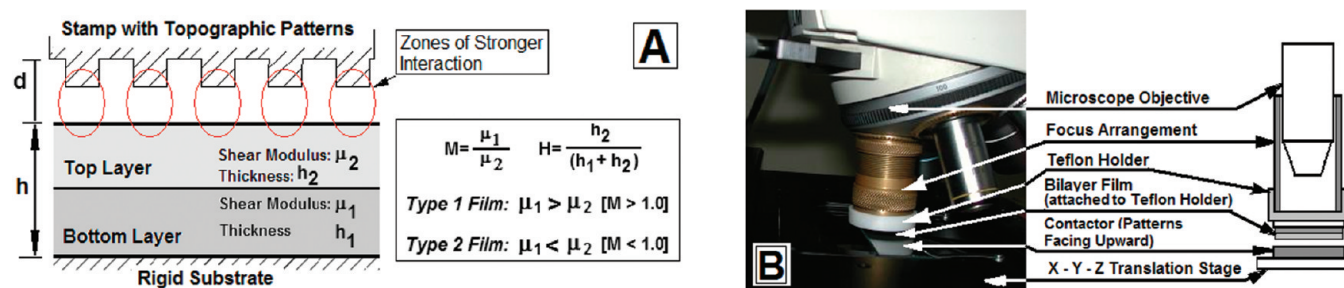


Figure 1. (A) Schematic of an elastic bilayer in proximity of a rigid patterned contactor before the onset of instability. The bottom film is bonded to a rigid surface. The highlighted locations on the film below the stamp protrusions experience higher adhesive force because of reduced inter-surface separation distance and become unstable first, resulting in directionality and alignment to the elastic instability patterns. (B) Digicam image with marking of the experimental setup used for in situ observations of contact instability of an elastic bilayers with a rigid, patterned stamp on an optical microscope platform.

a freely floating glassy polymer film subject to capillary forces imparted by a drop of water placed on it.⁵⁸ Further, the instability length scale in a liquid film is extremely sensitive to the precise nature of the confining field and the wavenumber cutoff is controlled exclusively by the stabilizing influence of surface tension.⁴³ In contrast, the elastic instability patterns exhibit a short-wave instability, the wavelength (λ) of which varies linearly with the film thickness ($\lambda \approx R_F h$). For a single-layer elastic film, $R_F \approx 3$. Interestingly, for relatively thick ($h \geq 1 \mu\text{m}$) films, λ is independent of all material properties like surface tension and the shear modulus of the film.^{2–15,22,29–32}

The elastic contact instability is important in various interfacial phenomena like adhesion, debonding and friction in soft films,⁹ nucleation and growth of crack in soft materials under confined geometries,³ peeling of pressure sensitive adhesives,¹¹ etc. Recently, self-organization during elastic contact instability has been utilized as a novel technique for patterning of soft polymer films.^{29–34} The method, which is known as elastic contact lithography (ECL),³⁰ relies on aligning the isotropic instability patterns by laterally confining them, either using a topographically patterned stamp,^{29–33} or a patterned substrate.³⁴ When a patterned stamp is used, the regions of the film under the stamp protrusions experience greater adhesive attraction, which leads to a periodic spatial variation in the level of interaction eventually resulting in lateral ordering of the instability patterns.^{29–33} In contrast, on a topographically patterned substrate, the coated film has an undulating top surface, and these undulations in contact proximity to a flat contactor result in the desired periodic spatial variation in the interaction between the film and the stamp, aligning the instability structures.³⁴ It is also reported that in ECL with a single film, the elastic instability structures follow their natural scaling of $\lambda \approx 3h$ rather strongly, even under lateral confinement.^{29–34} Further, depending on the commensuration between the λ and λ_p , it becomes possible to engineer a variety of complex patterns like an array of tiny holes, columns, double periodic stripes etc. using a patterned stamp or a substrate with simple 1D grating structure.^{30–34} Furthermore, the morphology of these patterns can be modulated by varying the stamp–film intersurface separation distance.^{22,29–34} It may be noted that a patterned confining mold has also been used to guide and align the wrinkles generated on the surface of a metal-capped polymer film upon heating the polymer above its glass transition temperature.⁵⁹ The relaxation of stresses generated because of a difference in the thermal expansion coefficients of the metal and polymer layer result in the wrinkles. However, in experiments involving

contact instability of an elastic film with a patterned stamp, the patterns do not form because of residual stresses but result from the destabilizing interaction or adhesive force imparted by the stamp itself.^{30–32}

The ability to create features that are distinct from the original stamp pattern, and their in situ modulation makes ECL rather distinct from standard soft lithography techniques.^{30–34} In most cases, the latter can produce a negative or (very rarely) a positive replica of the original stamp pattern.^{60–62} However, to exploit ECL as a truly versatile patterning technique, a greater flexibility on feature length scale beyond $\lambda \sim 3h$,^{2–15,22} is clearly desirable. It has been recently shown that additional controls on the pattern length scale can be gained ($\lambda \approx R_F h$, $R_F \neq 3$) in the contact instability of an elastic bilayer comprising of two stacked films with different thickness (h_1, h_2 ; thickness of bottom and top layers respectively) and shear moduli (μ_1, μ_2 ; shear modulus of bottom and top layers, respectively).^{1,35} Under appropriate conditions, it becomes possible to obtain pattern wavelengths (λ) that are smaller than the total film thickness ($R_F < 1$).¹ In general, contact instability of an elastic bilayer allows tuning of λ from short waves ($\sim 0.5h$) to long wave ($\sim 8h$), depending on three factors: (1) the ratio of the thickness of the two individual layers ($H = h_2/h$; $h = h_1 + h_2$); (2) the ratio of the shear moduli of the two layers ($M = \mu_1/\mu_2$); and (3) the stacking order.¹ It is seen that when a softer film is placed on top of a stiffer film ($\mu_1 > \mu_2$; $M > 1$), R_F is generally lower than 3 and can assume values as low as 0.5 under specific conditions.¹ On the other hand when a stiffer film is coated on top of a softer film ($\mu_1 < \mu_2$; $M < 1$), it results in values of R_F higher than 3.¹ Because miniaturization is desirable in most contexts and is often difficult to achieve, the situations where $R_F < 3$ are thus more attractive from the standpoint of patterning which essentially allows creation of finer structures from thicker films. Thus, a bilayer is the system of choice for patterning by ECL because of flexibility it can offer in controlling the feature size. This is in contrast to a single layer film where the pattern length scale is rather tightly restricted to $\lambda \approx 3h$. An earlier experimental study involving the contact instability of an elastic bilayer,¹ was performed with a flat contactor. The resulting patterns were of random shape and orientation, limiting their utility. Thus it becomes clear that the possible benefits of miniaturization and feature length scale control in an elastic bilayer can be utilized to the fullest extent for the generation of ordered mesoscale structures only when a topographically patterned contactor is used. In this article, we focus on the contact instability of an elastic bilayer system modulated by a patterned stamp, which is addressed for the first time. The

system is schematically shown in Figure 1A. We further show that the morphology of these patterns can be modulated by varying the vertical position of the stamp with respect to the film. We also show that the pattern morphology, which depends strongly on the commensuration of λ and λ_p , can be completely distinct from that of the original stamp and in some cases ordered 2D structures can be obtained using a stamp having strictly 1D features. While the creation of such 2D structures from an 1D stamp has earlier been reported with a single-layer films,^{29–33} the precise sequence of events that leads to formation of patterns which are completely distinct from the stamp pattern was never fully understood.^{30–33} Based on in situ optical microscopy we show here for the first time the precise evolution sequence that results in a secondary lateral instability after the formation of a positive replica of the stamp on the film surface, eventually transforming into an array of well ordered holes. We also show that by using a bilayer, values of R_F lower than 3 can be readily attained. It thus becomes possible to create fine features with sub-500 nm lateral resolution by ECL of an elastic bilayer, in contrast to a minimum lateral resolution of few micrometers achieved until now by ECL with a single-layer elastic film.^{30–34} Further, the elastic instability patterns, which are transient and exist only in proximity of the contactor, are made permanent by UV–ozone exposure, which results in oxidation and stiffening of the cross-linked PDMS film surface, making them permanent.^{30–34,63–65} Further, our experiments show that the surface energy of the stamp has no influence on the evolution process as well as on the final pattern morphology in ECL with a bilayer. This observation is theoretically anticipated^{1,4–7,35} and is also same as that observed in the ECL with a single layer film.^{30–32} Thus, the proposed technique of ECL with an elastic bilayer can be ideally suited for making defect free and large area (cm²) patterns with sub micrometer lateral resolutions at relatively low costs, and may find applications in patterning of soft coatings for the bulk-nano applications.

MATERIALS AND METHODS

Sylgard 184, a two part thermocurable poly dimethylsiloxane (PDMS) elastomer (Dow Corning, USA) consisting of an oligomer (part A) and a cross-linker is used to make both the constituent layers of the elastic bilayer. The films are spin coated from a dilute solution of Sylgard 184 in *n*-Heptane (HPLC grade, Merck, India). The shear modulus of the individual films is controlled by varying the cross-linker concentration. The thickness of the individual layers is controlled by varying the dilution of the coating solutions and spin speed (RPM). Thoroughly cleaned pieces of pure silica glass (quartz) slides (size 15 mm × 15 mm, both side polished, obtained from Applied Optics, India) are used as substrates. The use of quartz substrates is motivated by its transparency to UV light, which is necessary to make the patterns permanent.

In order to cast a bilayer, the bottom layer is first coated and cured at 120 °C for 12 h. Thermal annealing of Sylgard film results in physical cross-linking of the molecules. After curing, the thickness of this layer is measured by an imaging ellipsometer (ep3, Nanofilm, Germany) or by a mechanical profilometer (for thicker films). Subsequently, the second (top) layer with a different shear modulus is spin coated on the cross-linked bottom layer. After coating the second layer, the bilayer is again cured for 12 h at 120 °C to complete the cross-linking of the top layer as well. The total thickness of the bilayer is determined at this point by techniques mentioned before.

It is noted from literature that when $M = 9.15$, a significant lowering of R_F is seen over a rather wide range of H ($0.1 < H < 0.5$, Table 1). Therefore, for all the experiments reported in this paper, M has been maintained constant at 9.15. To obtain bilayer films with $M \approx 9.15$, the

Table 1. Values of H Used for Experiments and the Corresponding Values of R_F , Data Taken from Ref 1; $M = 9.15$

H	R_F
0.16	0.88
0.19	0.83
0.20	0.91
0.23	1.03
0.29	1.38
0.37	1.56
0.48	1.78
0.67	2.08
0.73	2.19

cross-linker concentration used for the bottom layer is 10% (part B: part A, wt/wt) and that for the top layer is 5%. The storage moduli (G') for the cured films with 5.0% and 10.0% cross-linker concentrations are $\sim 0.121 \pm 0.019$ and 1.108 ± 0.056 MPa, respectively, as obtained by the oscillatory parallel plate method (Bohlin rheometer). The corresponding loss moduli (G'') are 1.036 ± 0.011 and 8.219 ± 0.017 KPa, respectively. The values of H chosen for the samples in our experiments and the corresponding values of R_F , which are taken from available literature, are shown in Table 1.¹

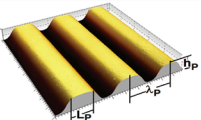
An AFM calibration grid and the polycarbonate part of commercially available optical data storage disks like CD and DVD are used as a rigid patterned contactor for the experiments. All the three stamps have a grating structure with a duty ratio of 1.0. The stamp periodicity (λ_p), line width (L_p), and stripe height (h_p) for the individual stamps are shown in Table 2. The polycarbonate part of the CD/DVD is isolated from the covering aluminum foil and cut into small pieces (15 × 15 mm²) for the experiments. The patterned pieces are washed in methanol to remove any impurity or pigment and subsequently dried in a stream of dry nitrogen before contact with the bilayer films. Details about the use of CD and DVD parts as low-cost stamps for patterning can be found in details elsewhere.^{65,66} The AFM calibration grid was silanized with Octadecyltrichlorosilane (OTS, Sigma Aldrich, UK) following standard procedure to facilitate detachment of the stamp after patterning.⁶⁷

The contact experiments are performed on the motorized X–Y–Z stage of an optical microscope (model DMLM, Leica), using a specially designed setup attached to the microscope objective which enables a fine movement in the Z direction, independent of the stage. A digicam image as well as a schematic of the setup with appropriate markings is shown in Figure 1B. The coated film is mounted at the bottom of this attachment, with the free surface of the film facing downward. The stamp is placed on the stage of the microscope, with its patterned surface facing toward the free surface of the film. The fine movement screw of the attachment and the Z-directional motion of the microscope stage is employed simultaneously in such a fashion so that when the stamp and the film come in proximity, the zone of contact remains in focus. Images are captured using a CCD camera mounted on to the microscope. Once in focus, the progressive approach of the stamp toward the film is controlled by the motorized Z movement screw of the stage.

The instability patterns originate due to an adhesive interaction between the stamp and the film, when they are in adhesive contact and disappear with the withdrawal of the stamp beyond a critical distance.^{1–15} To make the transient patterns permanent, we exposed the films to UV–ozone for 20 min, while in contact with the stamp. UV irradiation at 185 nm wavelength produces ozone from atmospheric oxygen, which subsequently dissociates to atomic oxygen at 254 nm irradiation.^{63,64} The atomic oxygen reacts with the silicone based cross-linked PDMS, forming a stiff surface layer of silicon oxide that prevents the relaxation of the film surface after stamp withdrawal, making the patterns permanent.^{30–34,63–65}

The following details of the sample preparation are also important. As the polymer and the solvent for both the layers are same (only the

Table 2. Details of the Patterned Stamps Used

Stamp Type	Stamp periodicity (λ_p)	Line width (L_p)	Stripe height (h_p)	Schematic Representation
AFM calibration grid	3.0 μm	1.5 μm	200 nm	
CD – Polycarbonate Part	1.5 μm	750 nm	120 nm	
DVD– Polycarbonate Part	800 nm	400 nm	70 nm	

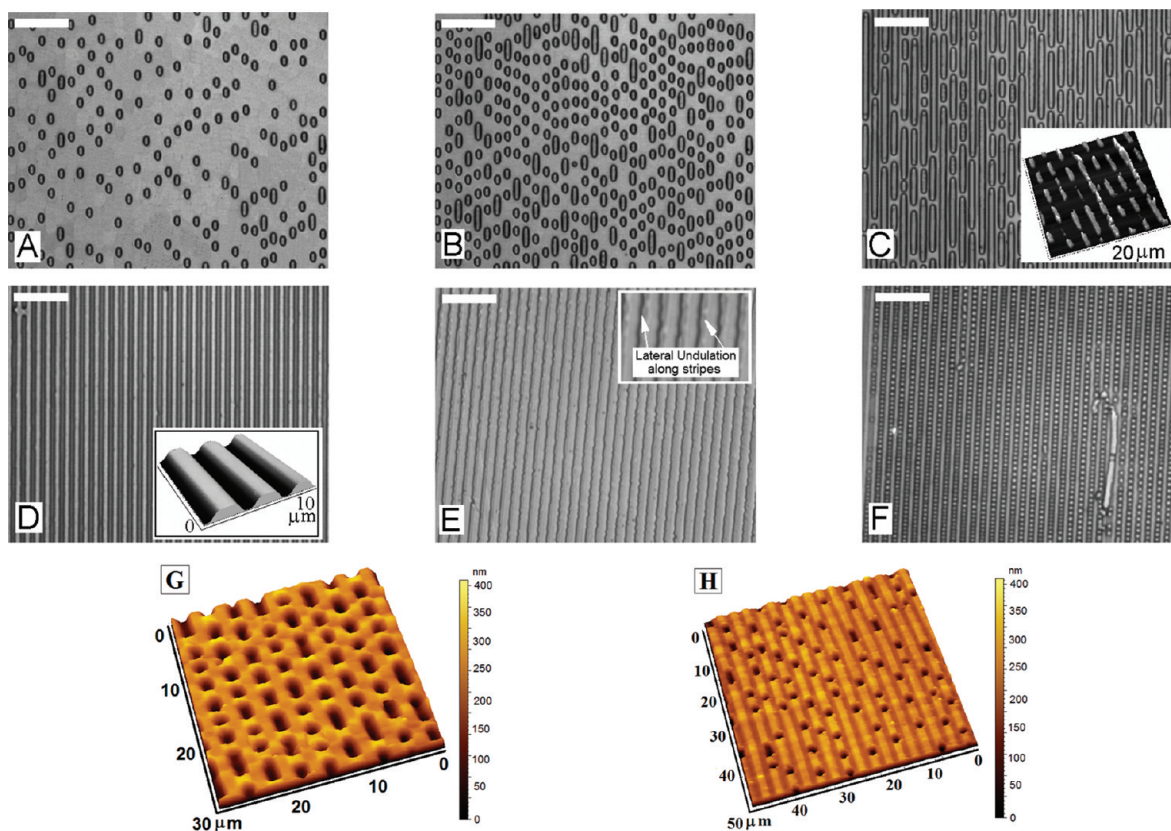


Figure 2. Morphological evolution sequence (frames A–H) of instability patterns in an elastic bilayer film having $h = 3.498 \mu\text{m}$; $M = 9.15$; $H = 0.16$ in proximity of a grating stamp with $\lambda_p = 3 \mu\text{m}$, $l_p = 1.5 \mu\text{m}$, and $h_p = 200 \text{ nm}$. In this case, $R_F = 0.88$ and $\lambda = 3.078 \mu\text{m}$. (A) Onset of instability is with isolated columns with nearly circular diameter; (B) more number of columns appear below the stamp protrusions; (C) stretched columns under stamp protrusions start joining up; (D) positive replica of the stamp pattern, with inset showing an AFM image of the structures made permanent at this stage; (E) undulations along the periphery of the stripes as the stamp approaches beyond the level of a positive replica formation, with inset showing the details; (F) aligned array of circular holes isolated by stripes, resulting from bridging of the secondary instability structures in the form of undulations on the stripe edges; (G) AFM image corresponding to the stage shown in F; (H) gradually disappearing holes leading to the formation of a perfect negative replica in the final stage of approach. The scale bar in all optical microscope images A–F corresponds to 15 μm .

cross-linker concentration is different), it is essential to ensure that the surface of the bottom (first) film is not damaged while spin coating the film. For this purpose the surface of the cured bottom film is initially scanned with an AFM (model 5100, Agilent Technologies), which shows the topography of the films to be flat with an rms roughness of $\sim 0.6 \text{ nm}$. Subsequently, instead of coating the second layer, few drops of pure *n*-heptane (solvent for Sylgard 184) is dispensed on the first film and spun using the spin coater. This step is identical to the coating of the second layer except no polymer is present. This gives the opportunity to examine if there is any solvent induced damage of the bottom film during the coating of the second layer. However, AFM scans after this step shows no statistically significant change in the rms roughness or topography of the film surface, which suggests that there is no dissolution of the bottom layer while coating the top layer, in presence of a common solvent. Thus, no damage or roughening of the film–film interface is expected (images shown in the Supporting Information, Figure S1), during coating of the top layer.

RESULTS AND DISCUSSIONS

When a topographically patterned stamp is brought in contact with a soft elastic bilayer, the zones of the film surface under the stamp protrusions (marked in figure 1A) experience higher attractive interaction and become unstable first contact. The spatial variation in the stamp – film interaction results in alignment of the instability patterns. Image sequence in figure 2, where a rigid silicon stamp (AFM calibration grid, $\lambda_p = 3.0 \mu\text{m}$) is brought in progressive contact with a bilayer ($h \approx 3.498 \mu\text{m}$, $H = 0.16$, $M = 9.15$, corresponding $R_F \approx 0.88$) shows how the morphology of the patterns continuously evolve with progressive approach of the stamp. For the sample shown in Figure 2, the bilayer parameters are chosen in such a way so that $\lambda (\approx 3.078 \mu\text{m})$ becomes very close to $\lambda_p (= 3.0 \mu\text{m})$.

Later in this article, we show the morphologies in cases where there is a mismatch between λ_p and λ .

During the approach of the patterned stamp, the onset of instability is manifested with the formation of discrete columns having circular cross-sections on the areas of the film below the stamp protrusions. The columns, which are aligned along the stripes, span between the film and the stamp (Figure 2A). As the contactor approaches further, reduced stamp–film separation results in an increased level of adhesion and as a result, more number of columns appears (Figure 2B). Concurrently, a reduction in the stamp–film gap results in compressing the preexisting columns as well, stretching them along the substrate stripes (Figure 2C). These stretched stripes on the film eventually merge with the neighboring ones under each stripe, forming a positive replica of the stamp pattern (Figure 2D). AFM scans (inset of Figure 2D) of patterns made permanent at this stage by UV ozone exposure shows that the height of the stripes is $\sim 351.6 \pm 3.3$ nm, which is much higher than the feature height of 200 nm on the stamp. This observation substantiates that the stripes are not a negative replica of the stamp resulting from imprinting, but a positive replica formed by elastic deformation of the film surface. It also becomes evident that engineering higher aspect ratio patterns is possible by ECL of an elastic bilayer.

When the contactor is allowed to approach further beyond the stage where a positive replica has already formed, the replicated stripes on the film further gets compressed, which in turn results in the formation of periodic undulations (Figure 2E) along the periphery (sides) of each stripe. The amplitude of these peripheral undulations, which is a secondary instability, grows further with progressive approach of the stamp (inset to Figure 2E), resulting in an adhesive interaction between the advancing undulation fronts facing each other, between every adjacent stripes. Eventually, these advancing undulation fronts grow and merge with each other, forming a bifurcated 2D secondary structures that periodically bridge the adjacent parallel stripes on the film surface. At this stage, the morphology of the patterns is an aligned array of tiny, nearly equal sized holes (femtoliter beakers) in the lateral direction that are isolated periodically in the transverse direction by stripes (Figure 2F). The AFM image in Figure 2G shows the detailed morphology of the holes and further reveals that the center to center distance of these holes along the direction of the stripes (λ_H) is $\sim 3.191 \pm 0.455$ μm , which is close to the instability length scale, λ (as well as λ_p). This shows that the bifurcation to 2D secondary instability patterns also follows the natural elastic instability length scale of the film. The periodic bridging between the undulating ridges leads to an increase in the contact area between the film and the stamp leading to the release of a higher degree of elastic strain energy. Subsequent reduction in the intersurface distance increasingly forms a negative replica of the stamp, with gradual disappearance of the holes and formation of the polymer ridges below the stamp valleys (Figure 2H). At this stage, the process becomes akin to imprint lithography in which the stamp sinks in the polymer. Experiments were also performed with films having identical composition and thickness, but with stamps with different surface energy (non silanized AFM grid, UVO exposed CD stamp, etc.), which reveal virtually no effect of the stamp surface energy on either the morphology of the structures or the evolution sequence. This suggests that even in a bilayer, the elastic contact instability wavelength is independent of the

adhesion strength, which is well-established for a single-layer film, both theoretically and experimentally.^{6,7,12,22,29–35}

In previously reported cases of ECL with a single film, it is seen that the secondary 2D patterns form only when there is a commensuration between λ and λ_p .^{30–33} This implies that for a given stamp with a specific λ_p , such patterns can be obtained only when $h \approx \lambda_p/3$. As the scaling factor R_F can be tailored for a bilayer, it becomes possible to obtain such ordered 2D patterns for a variety of film thickness, depending on the bilayer configuration (choice of H and M). In practice, this can be implemented by initially selecting H , and subsequently deciding the thickness of the individual layers in such a fashion that the product $R_F h$ becomes numerically close to λ_p (refer to image S2 in the Supporting Information). We would like to point out here that though all the results shown in this paper correspond to a value of $M = 9.15$, it is possible to obtain secondary instability induced ordered 2D structures for other values of M as well, which is also shown in the Supporting Information. The key message that emerges from these set of observations is: for a specific stamp, it becomes possible to obtain ordered 2-D structures with bilayers for variety of total film thickness (h), rather than restricting the film thickness to a specific value of $h \approx \lambda_p/3$, as in a single-layer film. The ability to obtain 2D structures with a thicker film in a bilayer adds significant flexibility to the technique of ECL and gains particular significance when a stamp with finer features (lower λ_p) is used, which is shown in the following example.

It has been shown by Gonuguntla et al. that in contact instability of a single layer elastic film, there is a nonlinear increase in the scaling factor R_F in films thinner than ~ 1 μm , because of enhanced influence of surface tension.²² Probably, as a result of this effect we have failed to obtain the ordered 2D patterns with a 500 nm and a 270 nm thick Sylgard film using a CD ($\lambda_p = 1.5$ μm) and a DVD ($\lambda_p = 800$ nm) stamp respectively, even though there is “apparent” commensuration between λ and λ_p based on the scaling relation of $\lambda = 3h$ for a single layer film. However, in reality, for films thinner than ~ 500 nm, R_F is seen to be ~ 6 or even higher.²² Thus, to have commensuration between λ and λ_p for a CD and a DVD stamp, ideally the film thickness (h) should be ~ 250 and 130 nm, respectively. However, Sylgard films thinner than ~ 300 nm are often not smooth and has isolated raised patches (image shown in the Supporting Information, Figure S3), the origin of which is attributed to the catalyst particles (typical diameter ~ 200 nm) present in the cross-linker (part B) of the Sylgard 184 itself.⁶⁸ When ECL is attempted with an ultrathin film, which is thinner than about 500 nm, these irregular clusters of particles act as spacers, hindering proper contact between the stamp and the film and as a result, hardly any pattern is obtained on the film surface. Thus, a combination of nonlinear increase of R_F and particle clusters acting as spacer in thinner films have prevented the creation of features with submicrometer lateral resolution by ECL until now, irrespective of the λ_p of the stamp. We show here that with an elastic bilayer, it becomes possible to overcome both of the limiting effects and achieve ordered 2D patterns with lateral resolution even lower than 500 nm. This can be seen in Figure 3, which shows an ordered 2D array of holes formed with a DVD stamp on a 940 nm thick elastic bilayer having $H \approx 0.20$ (corresponding $R_F \approx 0.91$ and $\lambda = 855$ nm) where the periodicity (λ_H) and diameter (d_H) of the holes is found to be $\sim 893 \pm 67$ and 357 ± 29 nm, respectively. This is the first example where features with sub-500 nm lateral resolution has been obtained by ECL, which has been possible

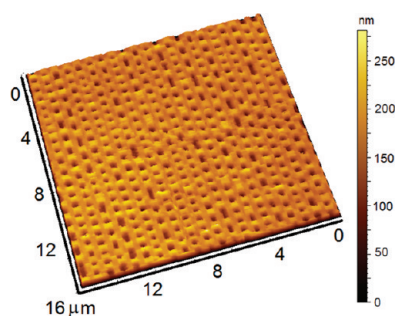


Figure 3. Ordered 2D structures in the form of array of femtoliter beakers formed on the surface of elastic bilayer films using a stamp having $\lambda_p = 800$ nm. The film thickness is 940 nm, $M = 9.15$ and $H = 0.21$. For this case, R_F is ~ 0.91 and the corresponding $\lambda = 853$ nm. The diameter of the holes is 357 ± 43 nm.

with the use of an elastic bilayer under specific cases where R_F has a value lower than 3. This enables the use of a thicker film which simultaneously overcomes the detrimental effects of surface tension induced enhancement of R_F as well as particle clusters acting as spacers in very thin films. It is possible that in bilayers with top layer thickness $< \sim 250$ nm (like the one shown in Figure 3), there can be some isolated particle clusters on the film surface. However, as these particles on the top layer are on a softer bottom layer, they (the particles) get pushed into the bottom layer when the rigid stamp approaches the film, allowing pattern formation. In case of a single-layer film coated on a rigid substrate, the particle cannot penetrate into the bottom layer and act as a spacer, hindering the pattern formation (refer to image S3 in the Supporting Information).

All the results presented thus far only correspond to the cases where λ_p is close to λ . Additional complexities arise when there is a mismatch between λ_p and λ , as elastic film tends to evolve on its natural instability length scale, λ even in the presence of a patterned contactor. This becomes clear from the following examples where we show the resulting morphologies for 3 different cases: case 1, where $\lambda < \lambda_p$; case 2, where λ and λ_p are very close to each other but are not exactly equal; and case 3, where $\lambda > \lambda_p$.

Figure 4A shows the final morphology for case 1, where an elastic bilayer with $h = 988$ nm, $H = 0.37$ ($R_F = 1.56$; $M = 9.15$, corresponding $\lambda \approx 1.541$ μm) is imprinted with an AFM calibration grid stamp having $\lambda_p = 3.0$ μm . In this case double periodic stripes with two raised ridges form below every protrusions of the stamp, which are further separated by an intervening channel. It shows that in case 1, specifically when λ is close to $\lambda_p/2$, it becomes possible to obtain self-organized features that have smaller lateral resolution than the original stamp periodicity (λ_p). Figure 4B shows another interesting morphology observed when a bilayer having $h = 1.060$ μm , $H = 0.29$ ($R_F = 1.38$; $M = 9.15$, corresponding $\lambda \approx 1.463$ μm) is imprinted with a CD stamp. In this case, λ is very close to, but slightly lower than λ_p (case 2). The resultant morphology partially resembles the structures observed when there is a perfect commensuration between λ_p and λ , but it can be seen in Figure 4B that the areas where the array of holes form are separated by a stripe which does not exhibit any secondary instability or lateral bridging. In order to explain the genesis of this complicated pattern, we have superimposed a schematic of the stamp and have individually indexed the protrusions to facilitate the discussion, on the AFM image in Figure 4B. It seems that in the initial stage of instability, a positive replica of the stamp pattern does indeed form on the film surface. However, as the stamp approaches further, the scenario becomes different from that seen in Figure 2G, where a secondary instability bridges all the adjacent stripes. In the present case, the bridging occurs between the stripes formed below protrusion numbers (1,2), (4,5), (7,8), etc., only and the stripes formed below the intervening protrusions, numbers 3 and 6, do not exhibit any secondary instability. Even in the stripes which exhibit secondary instability (below protrusion numbers 1, 2, 4, 5, 7, 8, etc.), the instability is manifested on only one side of them. Thus, the final morphology comprises alternate zones with ordered array of holes which are separated by stripes that do not participate in lateral bridging. Obtaining such highly complicated but well-ordered structures with multiple pattern length scale (periodicity of the holes, $\lambda_H \approx 1.459 \pm 0.057$ μm ; periodicity of the alternating zones exhibiting secondary instability as well as the intact stripes,

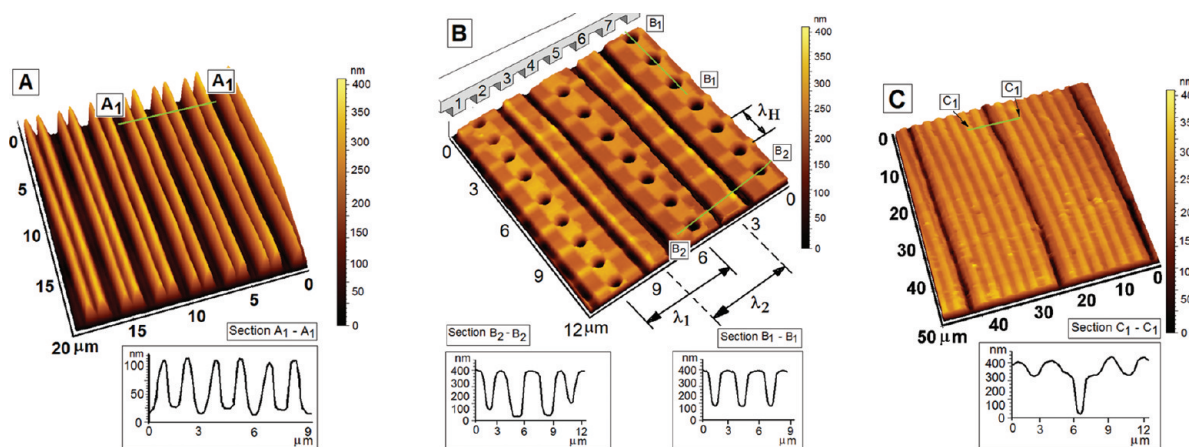


Figure 4. Morphology of the elastic instability patterns with bilayer films when the instability wavelength (λ) does not match the stamp periodicity (λ_p). (A) Multiple aligned structures under a stamp with wide protrusions, when elastic wavelength, λ , is approximately half of stamp periodicity, λ_p . Here, $h = 988$ nm, $H = 0.37$, $R_F = 1.56$, $\lambda_p = 3$ μm ; (B) unique multilength scale structure when is obtained when λ is very close but slightly lower than λ_p . The structure comprises of alternating zones having holes isolated by periodic stripes. Here $h = 1.060$ μm , $H = 0.29$, $R_F = 1.38$, $\lambda_p = 3$ μm ; (C) Imperfect replica with every 7th stripe missing forms when elastic instability length scale, λ is ~ 7 times larger than stamp periodicity, λ_p . Here $h = 9.81$ μm , $H = 0.67$, $R_F = 2.08$, $\lambda_p = 3$ μm .

marked as λ_1 and λ_2 respectively in Figure 4B, both = 3.0 μm) using a simple 1D grating stamp is rather novel. The possibility of obtaining somewhat similar multiperiodic patterns was theoretically predicted for an elastic film with a topographically patterned contactor (refer to Figure 20F in ref 29) by Sarkar et al., based on a complex energy minimization criterion which is found to depend on several parameters like the relative magnitudes of λ_p and λ and the stamp–film separation distance.²⁹ The occurrence of such alternating structures with multiple length scales can further be attributed to the existence of nontrivial bifurcation fields, the existence of which are already known for contact instability of a single layer elastic film as well as in the instability resulting from the interaction of two elastic films, which predicts that the region of instability is confined between two wavelengths. However, the precise conditions under which such complex yet extremely ordered structures can be obtained from a simple 1D stamp is yet to be fully understood theoretically. Experimentally, we find that the structures are reproducible, as they are obtained in several samples with stamps having different periodicities (we repeated the same experiment in at least six samples prepared in different batches). However, we must emphasize that this type of patterns are obtained only when λ_p and λ are very close to each other, with λ being slightly less than λ_p to within 8–10%. However, when the length scale commensuration is much better to within $\pm 5\%$, all the stripes undergo a secondary instability and morphologies similar to that shown in the Figure 2G results. Also morphologies similar to that shown in Figure 4B is never obtained when λ is slightly higher than λ_p , even if it falls within the 8–10% range.

Figure 4C shows the morphology when λ is higher than λ_p (case 3), where a bilayer with $h = 9.81 \mu\text{m}$, $H = 0.67$ ($R_F = 2.08$; $M = 9.15$, corresponding $\lambda \approx 20.38 \mu\text{m}$) is contacted with a stamp having $\lambda_p = 3 \mu\text{m}$. For this particular example, it can be seen that λ is roughly 7 times of λ_p . The resulting self-organized morphology also carries a clear signature of this relation ($\lambda = 7\lambda_p$) as every seventh stamp protrusion fails to produce a raised stripe on the film surface, as seen in Figure 4C. In this case, each broad ridge, spanning below six stamp protrusions and isolated by an intervening channel resulting from the missing seventh ridge, corresponds to one single elastic instability structure. It means the periodicity of these structures is 21 μm , which again correspond to the natural instability length scale for the specific bilayer. As can be seen from the figure, the top surface of each elastic instability structure (or broad ridge) contains an imprint of the stamp pattern, the height of which are $\sim 269 \text{ nm}$ (stamp height 200 nm), suggesting that these stripes are positive replicas of the stamp protrusions with which the stamp ridges establish a contact. This demonstrates how faithfully the resulting structures adhere to the elastic instability length scale in case 3, irrespective of the imposed lateral confinement. Thus, similar structures where every n th ridge gets missing can be easily created by choosing the values of h , H , and M in such a fashion that the corresponding λ simply becomes n times λ_p ($\lambda \approx n\lambda_p$). This aspect of the contact instability suggests yet another unique capability of manipulating the patterns morphology using the same stamp. Such flexibility is rather unprecedented in any other existing soft lithography technique.

CONCLUSIONS

We have shown that the random contact instability patterns (that form on a length scale λ) on the surface of a soft elastic

bilayer in contact proximity to another rigid surface can be aligned and modulated using a topographically patterned stamp with periodicity of λ_p . The use a bilayer allows creation of submicrometer pattern dimensions that has not been possible by using the contact instability of a single film. Further, depending on the commensuration (or the lack of it) between λ_p and λ , it becomes possible to create a variety of self-organized mesoscale structures. In addition to a positive or a negative replica of the stamp, more intricate self-organized patterns like double periodic channels, array of holes, alternating array of holes and stripes, columns, etc., can be fabricated using the same stamp. The patterns are also modulated by varying the contactor–film intersurface separation distance, which makes in situ reconfiguration of the patterns possible. Such ordered meso scale patterns in soft polymer can find wide variety of applications in various areas like structural super hydrophobicity, structural color applications, designing of micropatterned pressure sensitive adhesives, organic electronics and various types of confined chemistry and nano biotechnology applications. For example, the array of femto liter beakers (Figures 2G, 3, and 4B) can be used as nano reactors for synthesis of nano particles, single crystals etc.

Also, while the formation of regularly ordered 2D structures has been observed earlier in the context of ECL with a single layer film,^{29–32} the precise evolution sequence showing the progressive morphological transitions starting from the onset of instability with the appearance of an array of columns \rightarrow elongated columns \rightarrow positive replica \rightarrow 2D ordered array of holes \rightarrow negative replica is shown for the first time. Further, the use of a bilayer allows controlling the instability length scale λ by appropriate choice of H and M , making it possible to adjust the value of λ with respect to λ_p for a variety of bilayer thickness h . We have shown that this particular aspect can be utilized in successfully obtaining ordered features having submicrometer lateral resolution by overcoming the influence of surface tension and elastic stiffness induced increase in the scaling factor R_F for ultra thin films.²² The ability to achieve commensuration between λ and λ_p even in a thicker film also allows overcoming the problems associated in establishing a proper contact between the stamp and a very thin film ($\lesssim 500 \text{ nm}$) because of the presence of particle clusters on the film surface.

The possibility of engineering many distinct ordered patterns using a simple stamp having 1D features is indeed a notable aspect of elastic contact lithography with a bilayer. We term this as the Beyond the Master patterning because the proposed technique is not limited to creating a mere negative replica of the stamp pattern like most existing soft lithography techniques. Further, the method does not require major tools and instruments as necessary in many of the existing lithography methods.

ASSOCIATED CONTENT

Supporting Information

Additional figures (PDF). This material is available free of charge via the Internet at <http://pubs.acs.org>.

AUTHOR INFORMATION

Corresponding Author

*E-mail: rabibrata@iitkgp.ac.in (R.M.); ashutos@iitk.ac.in (A.S.).

ACKNOWLEDGMENTS

Discussions with Manoj Gonuguntla and Gaurav Tomar are gratefully acknowledged. This work was supported by the DST Unit on Soft Nanotechnology at IIT Kanpur and by an IRHPA grant of the DST, New Delhi.

REFERENCES

- (1) Mukherjee, R.; Pangule, R.; Sharma, A.; Tomar, G. *Adv. Funct. Mater.* **2007**, *17*, 2356.
- (2) Shull, K. R.; Flanagan, C. M.; Crosby, A. J. *Phys. Rev. Lett.* **2000**, *84*, 3057.
- (3) Crosby, A. J.; Shull, K. R.; Lakrout, H.; Creton, C. J. *Appl. Phys.* **2000**, *88*, 2956.
- (4) Ghatak, A.; Chaudhury, M. K.; Shenoy, V.; Sharma, A. *Phys. Rev. Lett.* **2000**, *85*, 4329.
- (5) Monch, W.; Herminghaus, S. *Europhys. Lett.* **2001**, *53*, 525.
- (6) Shenoy, V.; Sharma, A. *Phys. Rev. Lett.* **2001**, *86*, 119.
- (7) Shenoy, V.; Sharma, A. *J. Mech. Phys. Solids.* **2002**, *50*, 1155.
- (8) Webber, R. E.; Shull, K. R.; Roos, A.; Creton, C. *Phys. Rev. E* **2003**, *68*, 021805.
- (9) Sarkar, J.; Sharma, A.; Shenoy, V. *Langmuir* **2005**, *21*, 1457.
- (10) Ghatak, A.; Chaudhury, M. K. *Langmuir* **2003**, *19*, 2621.
- (11) Ghatak, A.; Mahadevan, L.; Chung, J. Y.; Chaudhary, M. K.; Shenoy, V. *Proc. R. Soc. London, Ser. A* **2004**, *460*, 2725.
- (12) Sarkar, J.; Shenoy, V.; Sharma, A. *Phys. Rev. Lett.* **2004**, *93*, 018302.
- (13) Ghatak, A. *Phys. Rev. E* **2006**, *73*, 041601.
- (14) Sarkar, J.; Sharma, A. *Langmuir* **2010**, *26*, 8464.
- (15) Ghatak, A. *Phys. Rev. E* **2010**, *81*, 021603.
- (16) Ru, C. Q. *J. Appl. Phys.* **2001**, *90*, 6098.
- (17) Shenoy, V.; Sharma, A. *Langmuir* **2002**, *18*, 2216.
- (18) Sarkar, J.; Sharma, A.; Shenoy, V. *Phys. Rev. E* **2003**, *67*, 031607.
- (19) Yoon, J.; Ru, C. Q.; Midouchowski, A. *J. Appl. Phys.* **2005**, *98*, 113503.
- (20) Chung, J. Y.; Chaudhury, M. K. *J. Adhes.* **2005**, *81*, 1119.
- (21) Chung, J. Y.; Kim, K. H.; Chaudhury, M. K.; Sarkar, J.; Sharma, A. *Eur. Phys. J. E* **2006**, *20*, 47.
- (22) Gonuguntla, M.; Sharma, A.; Sarkar, J.; Subramanian, S. A.; Ghosh, M.; Shenoy, V. *Phys. Rev. Lett.* **2006**, *97*, 018303.
- (23) Huang, S.; Li, Q.; Feng, X.; Yu, S. *Mech. Mater.* **2006**, *38*, 88.
- (24) He, L. H.; Lim, C. W. *Int. J. Solids Struct.* **2006**, *43*, 132.
- (25) Hui, C. Y.; Glassmaker, N. J.; Tang, T.; Jagota, A. *J. R. Soc., Interface* **2004**, *1*, 35.
- (26) Golovin, A. A.; Davis, S. H.; Voorhees, P. W. *Phys. Rev. E* **2003**, *68*, 056203.
- (27) Golovin, A. A.; Levine, M. S.; Savina, T. V.; Davis, S. H. *Phys. Rev. B* **2004**, *70*, 235342.
- (28) Matsumoto, E. A.; Kamien, R. D. *Phys. Rev. E* **2009**, *80*, 021604.
- (29) Sarkar, J.; Sharma, A.; Shenoy, V. *J. Adhes.* **2005**, *81*, 271.
- (30) Gonuguntla, M.; Sharma, A.; Mukherjee, R.; Subramanian, S. A. *Langmuir* **2006**, *22*, 7066.
- (31) Sharma, A.; Gonuguntla, M.; Mukherjee, R.; Subramanian, S. A.; Pangule, R. C. *J. Nanosci. Nanotechnol.* **2007**, *7*, 1744.
- (32) Gonuguntla, M.; Sharma, A.; Subramanian, S. A. *Macromolecules* **2006**, *39*, 3365.
- (33) Pangule, R. C.; Banerjee, I.; Sharma, A. *J. Chem. Phys.* **2008**, *128*, 234708.
- (34) Mukherjee, R.; Pangule, R. C.; Sharma, A.; Banerjee, I. *J. Chem. Phys.* **2007**, *127*, 064703.
- (35) Tomar, G.; Sharma, A.; Shenoy, V.; Biswas, G. *Phys. Rev. E* **2007**, *76*, 011607.
- (36) Arun, N.; Sharma, A.; Shenoy, V.; Narayan, K. S. *Adv. Mater.* **2006**, *18*, 660.
- (37) Arun, N.; Sarkar, J.; Sharma, A.; Shenoy, V.; Narayan, K. S. *J. Adhes.* **2007**, *83*, 513.
- (38) Sarkar, J.; Sharma, A. *Phys. Rev. E* **2008**, *77*, 031604.
- (39) Arun, N.; Sharma, A.; Pattader, P. S. G.; Banerjee, I.; Dixit, H. M.; Narayan, K. S. *Phys. Rev. Lett.* **2009**, *102*, 254502.
- (40) Pattader, P. S. G.; Banerjee, I.; Sharma, A.; Bandyopadhyay, D. *Adv. Funct. Mater.* **2011**, *21*, 324.
- (41) Ruckenstein, E.; Jain, R. K. *J. Chem. Soc., Faraday Trans. II* **1974**, *70*, 132.
- (42) Reiter, G. *Phys. Rev. Lett.* **1992**, *68*, 75.
- (43) Sharma, A.; Reiter, G. *J. Colloid Interface Sci.* **1996**, *178*, 383.
- (44) Sharma, A.; Khanna, R. *Phys. Rev. Lett.* **1998**, *81*, 3463.
- (45) Xie, R.; Karim, A.; Douglas, J. F.; Han, C. C.; Weiss, R. A. *Phys. Rev. Lett.* **1998**, *81*, 125.
- (46) Mukherjee, R.; Gonuguntla, M.; Sharma, A. *J. Nanosci. Nanotechnol.* **2007**, *7*, 2069.
- (47) Sehgal, A.; Ferreira, V.; Douglas, J. F.; Amis, E. J.; Karim, A. *Langmuir* **2002**, *18*, 7041.
- (48) Mukherjee, R.; Bandyopadhyay, D.; Sharma, A. *Soft Matter* **2008**, *4*, 2086.
- (49) Schaffer, E.; Thurn-Albrecht, T.; Russel, T. P.; Steiner, U. *Nature* **2000**, *403*, 874.
- (50) Voicu, N. E.; Harkema, S.; Steiner, U. *Adv. Funct. Mater.* **2006**, *16*, 926.
- (51) Schaffer, E.; Harkema, S.; Roerdink, M.; Blossey, R.; Steiner, U. *Macromolecules* **2003**, *36*, 1645.
- (52) Schaffer, E.; Harkema, S.; Roerdink, M.; Blossey, R.; Steiner, U. *Adv. Mater.* **2003**, *15*, 514.
- (53) Reiter, G.; Hamieh, M.; Damman, P.; Slavovs, S.; Gabriele, S.; Vilmin, T.; Raphaël, E. *Nat. Mater.* **2005**, *4*, 754.
- (54) Gabriele, S.; Damman, P.; Slavovs, S.; Desprez, S.; Coppee, S.; Reiter, G.; Hamieh, M.; Al Akhrass, S.; Vilmin, T.; Raphael, E. *J. Polym. Sci. B* **2006**, *44*, 3022.
- (55) Sharma, A.; Mittal, J. *Phys. Rev. Lett.* **2001**, *89*, 186101.
- (56) Saffman, P. G.; Taylor, G. I. *Proc. R. Soc. London, Ser. A* **1958**, *245*, 312.
- (57) Tietzel, M.; Troian, S. M. *Phys. Rev. Lett.* **2009**, *103*, 074501.
- (58) Huang, J.; Juszkiewicz, M.; de Jeu, W. H.; Cerda, E.; Emrick, T.; Menon, N.; Russell, T. P. *Science* **2007**, *317*, 650.
- (59) Yoo, P. J.; Park, S. Y.; Kwon, S. J.; Suh, K. Y.; Lee, H. H. *Appl. Phys. Lett.* **2003**, *83*, 4444.
- (60) Xia, Y.; Whitesides, G. M. *Angew. Chem., Int. Ed.* **1998**, *37*, 550.
- (61) Chou, S. Y.; Krauss, P. R.; Renstrom, P. J. *Appl. Phys. Lett.* **1995**, *67*, 3114.
- (62) Suh, K. Y.; Kim, Y. S.; Lee, H. H. *Adv. Mater.* **2001**, *13*, 1386.
- (63) Bowden, N.; Brittain, S.; Evans, A. G.; Hutchinson, J. W.; Whitesides, G. M. *Nature* **1998**, *393*, 146.
- (64) Efimenko, K.; Wallace, W. E.; Genzer, J. J. *Colloid Interface Sci.* **2002**, *254*, 306.
- (65) Mukherjee, R.; Sharma, A.; Gonuguntla, M.; Patil, G. K. *J. Nanosci. Nanotechnol.* **2008**, *8*, 3406.
- (66) Mukherjee, R.; Patil, G. K.; Sharma, A. *Ind. Eng. Chem. Res.* **2009**, *48*, 8812.
- (67) Wasserman, S. R.; Tao, Y. T.; Whitesides, G. M. *Langmuir* **1989**, *5*, 1074.
- (68) Kim, J.; Chaudhury, M. K.; Owen, M. J. *IEEE Trans. Dielectr. Electr. Insulation* **1999**, *6*, 695.